

Nanotip formation on a carbon nanotube pillar array for field emission application

Padmnabh Rai, Dipti R. Mohapatra, K. S. Hazra, D. S. Misra, and S. P. Tiwari

Citation: *Applied Physics Letters* **93**, 131921 (2008); doi: 10.1063/1.2996283

View online: <http://dx.doi.org/10.1063/1.2996283>

View Table of Contents: <http://scitation.aip.org/content/aip/journal/apl/93/13?ver=pdfcov>

Published by the [AIP Publishing](#)

Articles you may be interested in

[Field-emission properties of carbon nanotubes grown using Cu–Cr catalysts](#)

J. Vac. Sci. Technol. B **27**, 41 (2009); 10.1116/1.3039691

[ZnO nanoparticle growth on single-walled carbon nanotubes by atomic layer deposition and a consequent lifetime elongation of nanotube field emission](#)

Appl. Phys. Lett. **90**, 263104 (2007); 10.1063/1.2745226

[High-current-density field emission from multiwalled carbon nanotubes by chemical-vapor deposition with effective aging treatment](#)

J. Vac. Sci. Technol. B **25**, 583 (2007); 10.1116/1.2717199

[Polymer supported carbon nanotube arrays for field emission and sensor devices](#)

Appl. Phys. Lett. **89**, 103113 (2006); 10.1063/1.2345615

[Vertically aligned carbon nanotube field emission devices fabricated by furnace thermal chemical vapor deposition at atmospheric pressure](#)

J. Vac. Sci. Technol. B **24**, 1190 (2006); 10.1116/1.2190671

An advertisement for Keysight B2980A Series Picoammeters/Electrometers. It features a red and white background with a ruler-like scale at the top. The text reads: 'Confidently measure down to 0.01 fA and up to 10 PΩ' and 'Keysight B2980A Series Picoammeters/Electrometers'. Below the text is a small image of the device and the Keysight Technologies logo. A red button with white text says 'View video demo >'.

Confidently measure down to 0.01 fA and up to 10 PΩ
Keysight B2980A Series Picoammeters/Electrometers
View video demo >



Nanotip formation on a carbon nanotube pillar array for field emission application

Padmnabh Rai,¹ Dipti R. Mohapatra,¹ K. S. Hazra,¹ D. S. Misra,^{1,a)} and S. P. Tiwari²

¹Department of Physics, Indian Institute of Technology Bombay, Mumbai-400 076, India

²Department of Electrical Engineering, Indian Institute of Technology Bombay, Mumbai-400 076, India

(Received 12 August 2008; accepted 10 September 2008; published online 3 October 2008)

The field emission of a carbon nanotube (CNT) pillar array has been improved significantly by plasma treatment in a mixture of hydrogen and nitrogen gases. The plasma treatment for 30 s on a pillar array decreased the turn-on electric field from 0.48 to 0.37 V/ μm and increased the field enhancement factor from 6200 to 6900. The emission current density increased by a factor of ≈ 40 . We report in this letter the technique of generating nanotips on CNT pillars with an enormous potential to become a tool for the control and manipulation of CNTs and nanostructures. © 2008 American Institute of Physics. [DOI: 10.1063/1.2996283]

Carbon nanotubes (CNTs) have proved to be an ideal field emitting material due to their high aspect ratio, high electrical conductivity, high mechanical strength, and chemical inertness.^{1–5} For display applications, CNT films are preferentially obtained by chemical vapor deposition (CVD) techniques,⁶ the main advantage of CVD being the direct growth of the nanotube film emitter onto the substrate which can be further used as a cathode. The CNT pillar array has proved to be a better field emitter than the CNT film due to the reduced screening effect and enhancement in field due to the edge effect.^{7–10} The surface treatment of as grown CNT films has also proven to be an effective way to enhance the field emission property.^{11–15} Zhi *et al.*¹¹ used hydrogen (H_2) plasma treatment to enhance the emission current density of CVD grown CNTs. The enhancement was attributed to the formation of $\text{C}^{-\delta}-\text{H}^{+\delta}$ dipole layer on the CNT surface, tip sharpening, and increase in defect density. Gohel *et al.*¹² argued that the enhancement in the emission current density after nitrogen (N_2) plasma treatment occurs both due to physical and chemical changes that take place during the treatment. In physical changes, the N_2 plasma causes the CNT density to decrease and the nanotube length to be shortened, and the chemical changes occur due to N_2 doping in CNT films during plasma treatment. In recent years, a few groups have also reported that the work function of amorphous carbon films^{16,17} can be reduced by incorporating nitrogen into the films.

In this letter, we report a method of transforming the CNT pillar arrays into a conical shaped emitter array by plasma treatment in a plasma of a mixture of H_2 and N_2 gases. The pillar arrays have been fabricated on a patterned silicon wafer by thermal CVD technique. The conical needles formed after the plasma treatment, of almost perfect shape, are found to be excellent field emitters. This is evident from an enhancement observed in the emission current density by a factor of ≈ 40 after the plasma treatment. The improved emission current density is attributed to enhancement in the field at the tip of the emitter, reduction in screening effect, and increase in the aspect ratio.

Aligned CNT pillar array samples were synthesized by thermal CVD on the patterned silicon wafer. The patterns of

circular cross section of 200 μm diameter of silicon oxide (thermally grown 50 nm thickness) were fabricated on silicon wafer by photolithography in a matrix of chrome-gold (Cr/Au). Cr/Au layer is used to prevent the growth of CNTs on locations other than the silicon oxide. The experimental procedure for the growth of CNTs by thermal CVD process is described elsewhere.¹⁸ The plasma treatment of as grown CNT pillar array was carried out in a plasma of a mixture of H_2 and N_2 gases generated by microwave power. The flow rates of H_2 and N_2 were 40 and 10 SCCM (SCCM denotes cubic centimeter per minute at STP), respectively. The operating temperature, pressure, and process duration for the plasma treatment were 600 °C, 10 Torr, and 30 s, respectively. The structural and chemical modifications of CNTs arrays before and after the plasma treatment were examined by a Hitachi model S3400N scanning electron microscope (SEM) and Jobin Yvon model HR800 micro-Raman spectrometer, respectively. The field emission characteristics of the sample before and after plasma treatment were measured in a high vacuum chamber with a parallel diode-type configuration at a base pressure of $\sim 5 \times 10^{-7}$ mbar. The field emission current was measured at different voltages using an automatically controlled Keithley 6514 electrometer and power supply (model SRS, PS-325).

Figure 1 shows the SEM micrographs of the as grown CNT pillar array as well as the conical shaped CNT pillars after the plasma treatment for 30 s. Figures 1(a) and 1(b) show the CNT pillar array before the plasma treatment. A high degree of alignment between the adjacent CNT pillars is seen. It can be seen from Figs. 1(a) and 1(b) that the typical diameter and spacing between the two pillars are 200 μm and 2 mm, respectively. Figures 1(c) and 1(d) show the conical shaped pillars after the plasma treatments. The pillars of circular cross section are converted into almost perfectly shaped cones. The top diameter of the conical shape CNT pillar after the treatment is $\approx 30\text{--}40$ μm , as measured using SEM. It is possible, however, that the tip radius may be smaller than reported here. It is observed that the distance between the pillars increases after the plasma treatment. The plasma etching rates in the vertical and horizontal directions are approximately 10 and 5 $\mu\text{m/s}$, respectively. The etching of the pillar in the corner region is likely to be substantially higher than that in the central region because the corners will

^{a)}Electronic mail: nirdesh@phy.iitb.ac.in.

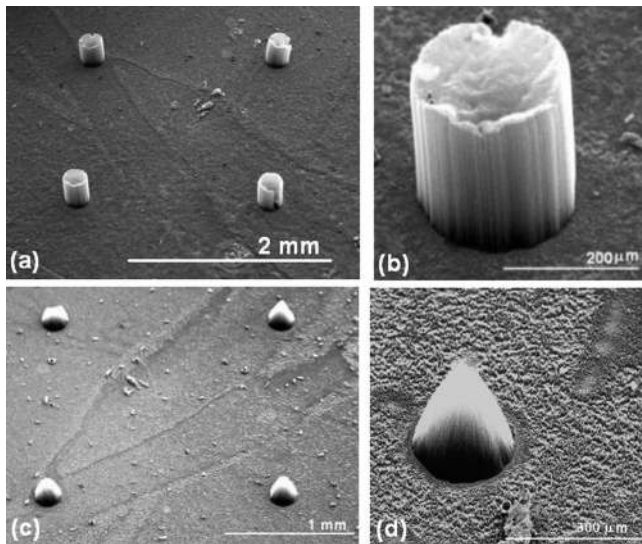


FIG. 1. (a) A SEM overview image of an as grown CNT pillar array. (b) Magnified image of an as grown CNT pillar. (c) SEM micrograph of a $H_2 + N_2$ plasma treated CNT pillar array. Plasma treatment changes the shape of the pillar into a cone. (d) Magnified overview of a conical shape CNT bunch.

contain a higher density of pentagon/octagon defects. In the central part of the pillars, the defect density will be low due to entangling. As we expose the pillar array in plasma, the anisotropy of the etching rate in the vertical and horizontal directions converts the pillar into a conical shape after a certain time.

The Raman spectra of the CNT pillar array before and after plasma treatment in the frequency range of $1000\text{--}2000\text{ cm}^{-1}$ are shown in Fig. 2. The spectra show mainly two Raman bands at 1350 cm^{-1} (D band) and 1580 cm^{-1} (G band). In the spectra of CNT pillar array, the D' band appears as a small shoulder of the G band at 1610 cm^{-1} . The origin of the D and D' bands have been attributed as the disorder features of graphitic sheets.¹⁹ The D and D' bands become stronger and sharper after plasma treatment. The details of the Raman analysis is summarized in Table I. The values given in parentheses in Table I are the full width at half maximum (FWHM) of the corresponding peaks. The intensity ratio of the D band to the G band

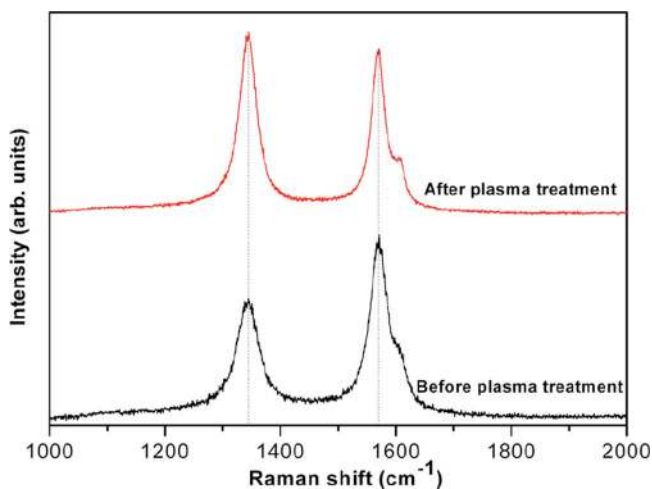


FIG. 2. (Color online) The Raman spectra of an as grown and CNT pillar array after $H_2 + N_2$ plasma treatment.

TABLE I. Summary of Raman spectra for an as grown and CNT pillar array after $H_2 + N_2$ plasma treatment.

Sample	D band (cm^{-1})	G band (cm^{-1})	D' band (cm^{-1})	I_D/I_G
As grown	1344 (38)	1570 (33)	1605 (20)	0.79
Plasma treated	1344 (32)	1569 (26)	1606 (17)	1.07

(I_D/I_G) increased from 0.79 to 1.09 after plasma treatment. The decrease in FWHM of the D band is indicative of the decreased sp^2 character, while the sharpening of the G band may be due to the removal of amorphous carbon from the surface of the nanotube.

Figure 3 shows the results of the field emission measurement made on the as grown CNT pillar array as well as the conical shape CNT pillar array after plasma treatment. The turn-on fields (defined at an emission current density of $10\text{ }\mu\text{A}/\text{cm}^2$) for the sample before and after plasma treatment are 0.48 and $0.37\text{ V}/\mu\text{m}$, respectively. The maximum emission current density drawn at a field of $0.63\text{ V}/\mu\text{m}$ increased significantly from a mere $3\text{ to }115\text{ mA}/\text{cm}^2$ after the plasma treatment. In order to obtain stable and reproducible field emission characteristics, high currents were generated initially between the anode and CNT pillar array to remove any adsorbates and burn out the loosely attached nanotubes on the top surface. The emission current followed the Fowler–Nordheim (FN) law, where the current density J is related to the applied electric field E as $J = A(\beta^2 E^2 / \varphi) \exp(-B\varphi^{3/2} / \beta E)$, where $A = 1.56 \times 10^{-6}\text{ A V}^{-2}\text{ eV}$, $B = 6.83 \times 10^7\text{ eV}^{-3/2}\text{ V cm}^{-1}$, β is the field enhancement factor, φ is the work function (eV), and E is the applied electric field in $\text{V}/\mu\text{m}$. The inset in Fig. 3 shows the linear FN behavior, indicating a field emission signature from the CNT pillar array. The curves (FN plots) show two linear regions with a knee point in between, one in the low field region and another in the high field region, which are denoted by I and II, respectively. The appearance of a knee point in the FN plots may be due to heating of the CNT top surface²⁰ as well as the rate limiting step for emission²¹ in the high field region. Recently, a few experiments have shown that there is an enhancement in the emission current with the increase in the CNT substrate (surface) temperature.²² This phenomenon has been explained in the

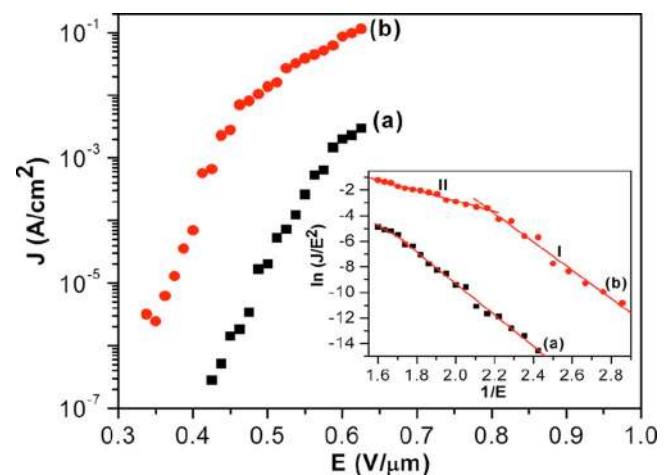


FIG. 3. (Color online) Field emission current density vs electric field for a vertically aligned CNT pillar array (a) before and (b) after $H_2 + N_2$ plasma treatment. The inset is the corresponding FN plots.

terms of a change in work function ϕ of the CNTs.²² We have used the value of work function of ≈ 5 eV for CNTs to calculate the field enhancement factor. The estimated field enhancement factors in the low field region are 6200 and 6900, whereas in the high field region, the values are 8400 and 18 700 for the sample before and after plasma treatment, respectively. The dramatic increase in the enhancement factor in the high field region of the FN plot for the plasma treated sample may be due to protrusion of more CNTs in the high field.

The enhanced field emission after the plasma treatment is attributed to the decrease in the pillar density and the transformation of the pillars into a perfect conical shape with shortened height. This reduces the screening effect and enhances the field amplification factor.⁸ The sharpening of the pillar tip additionally enhances the field amplification factor because the geometrical enhancement factor would amplify highly due to the formation of a sharp conical tip. The chemical changes may be occurring due to incorporation of H₂ and N₂ in CNTs. The H₂ incorporation will form the C–H dipole layer on the CNT surface.¹¹ The potential drop across the dipole layer may raise the surface band energy, resulting in a reduction in the electron affinity and enhance the field emission property of the CNTs accordingly. The N₂ doping may reduce the work function of the CNTs and increase their metallic character to effectively improve the field emission property.¹²

The increase in the I_D/I_G ratio indicates the increasing of the defects in the CNT pillar array after plasma treatment. Calculation showed that the field enhancement factor of the body is about 1/125 of the tip with the same radius.²³ The emission probability of the electrons at the tip should be much larger than those at the body due to the geometrical effect. Both experimental¹ and theoretical²⁴ studies have shown that the tip as well as the defects on the CNTs have predominant effects on the field emission of the CNTs. Zhou *et al.*²⁴ showed that for the local emission regions at the tip, the local density of states peaks on both sides of the Fermi level, corresponding to the donor and acceptor states, resulting in a remarkable shift to the Fermi level in comparison to that of in the body due to the presence of a conventional topographic defect.

In conclusion, the field emission behaviors of CNT pillar arrays treated with a plasma of a mixture of H₂ and N₂ gases is investigated systematically. The enhanced field emission of the array after the treatment is attributed to the physical

changes in CNT pillar array by plasma treatment such as enhancement in the geometrical factor due to the conical shape, reduction in the screening effect, and structural and chemical changes in the CNTs. Our results indicate that the plasma treatment described in this letter has enormous potential for the control and manipulation of CNTs and related nanostructures.

¹A. G. Rinzler, J. H. Hafner, P. Nikolaev, L. Lou, S. G. Kim, D. Tomanec, P. Nordlander, D. T. Colbert, and R. E. Smalley, *Science* **269**, 1550 (1995).

²W. A. Dee Heer, A. Chatelain, and D. A. Ugarte, *Science* **270**, 1179 (1995).

³Q. H. Wang, T. D. Corrigan, J. Y. Dai, R. P. H. Chang, and A. R. Krauss, *Appl. Phys. Lett.* **70**, 3308 (1997).

⁴A. M. Rao, D. Jacques, R. C. Haddon, W. Zhu, C. Bower, and S. Jin, *Appl. Phys. Lett.* **76**, 3813 (2000).

⁵H. Murakami, M. Hirakawa, C. Tanaka, and H. Yamakawa, *Appl. Phys. Lett.* **76**, 1776 (2000).

⁶R. Andrews, D. Jacques, A. M. Rao, F. Derbyshire, D. Qian, X. Fan, E. C. Dickey, and J. Chen, *Chem. Phys. Lett.* **303**, 467 (1999).

⁷S. Fan, M. G. Chapline, N. R. Franklin, T. W. Tombler, A. M. Cassell, and H. Dai, *Science* **283**, 512 (1999).

⁸V. Semet, V. T. Binh, P. Vincent, D. Guillot, K. B. K. Teo, M. Chhowalla, G. A. J. Amartunga, W. I. Milne, P. Legagneux, and D. Pribat, *Appl. Phys. Lett.* **81**, 343 (2002).

⁹S. Fujii, S.-I. Honda, H. Machida, H. Kawai, K. Ishida, M. Katayama, H. Furuta, T. Hirao, and K. Oura, *Appl. Phys. Lett.* **90**, 153108 (2007).

¹⁰J. L. Killian, N. B. Zuckerman, D. L. Neimann, B. P. Ribaya, M. Rahman, R. Espinosa, M. Meyyappan, and C. V. Nguyen, *J. Appl. Phys.* **103**, 064312 (2008).

¹¹C. Y. Zhi, X. D. Bai, and E. G. Wang, *Appl. Phys. Lett.* **81**, 1690 (2002).

¹²A. Gohel, K. C. Chin, Y. W. Zhu, C. H. Sow, and A. T. S. Wee, *Carbon* **43**, 2530 (2005).

¹³S. J. Kyung, J. B. Park, J. H. Lee, and G. Y. Yeom, *J. Appl. Phys.* **100**, 124303 (2006).

¹⁴T. Feng, J. Zhang, Q. Li, X. Wang, K. Yu, and S. Zou, *Physica E (Amsterdam)* **36**, 28 (2007).

¹⁵W. S. Kim, H. Oki, A. Kinoshita, K. Murakami, S. Abo, F. Wakaya, and M. Takai, *J. Vac. Sci. Technol. B* **26**, 760 (2008).

¹⁶B. S. Satyanarayana, J. Roberston, and W. I. Milne, *J. Appl. Phys.* **87**, 3126 (2000).

¹⁷A. Llie, A. Hart, A. J. Flewitt, J. Roberston, and W. I. Milne, *J. Appl. Phys.* **88**, 6002 (2000).

¹⁸P. Rai, D. R. Mohapatra, K. S. Hazra, D. S. Misra, J. Ghatak, and P. V. Satyam, *Chem. Phys. Lett.* **455**, 83 (2008).

¹⁹P. C. Eklund, J. M. Holden, and R. A. Jishi, *Carbon* **33**, 959 (1995).

²⁰S. K. Patra and G. M. Rao, *J. Appl. Phys.* **100**, 024319 (2006).

²¹R. C. Smith, J. D. Carey, R. J. Murphy, W. J. Blau, J. N. Coleman, and S. R. P. Silva, *Appl. Phys. Lett.* **87**, 263105 (2005).

²²C. M. Tan, J. Jia, and W. Yu, *Appl. Phys. Lett.* **86**, 263104 (2005).

²³G. Zhou, W. H. Duan, and B. L. Gu, *Appl. Phys. Lett.* **79**, 836 (2001).

²⁴G. Zhou, W. H. Duan, and B. L. Gu, *Phys. Rev. Lett.* **87**, 095504 (2001).